Supporting information for: Ribozyme catalysis with a twist: the active state of the twister ribozyme in solution predicted from molecular simulation

Colin S. Gaines and Darrin M. York*

Center for Integrative Proteomics Research, BioMaPS Institute and Department of Chemistry & Chemical Biology, Rutgers University, 174 Frelinghuysen Road, Piscataway, NJ 08854-8076, USA

E-mail: york@biomaps.rutgers.edu

*To whom correspondence should be addressed

Supplementary Figures

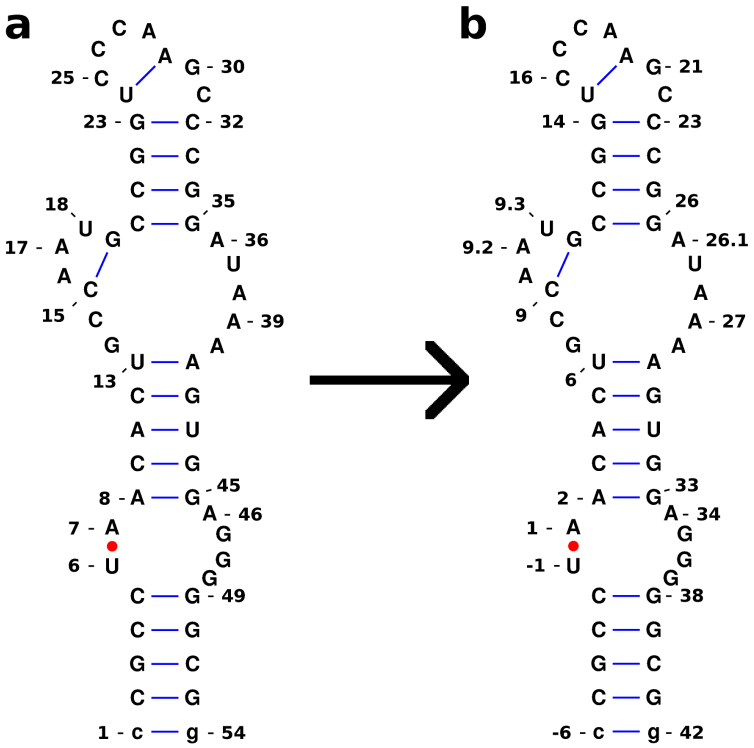

Figure S1: Mapping of residues numbered in order of appearance (a) in PDBID: 4OJI to numbering scheme (b) starting from the scissile phosphate marked by the red dot, in order to be generally independent of sequence length for the twister ribozyme. NB: base pairs invloved in forming the two pseudoknots not shown for clarity.

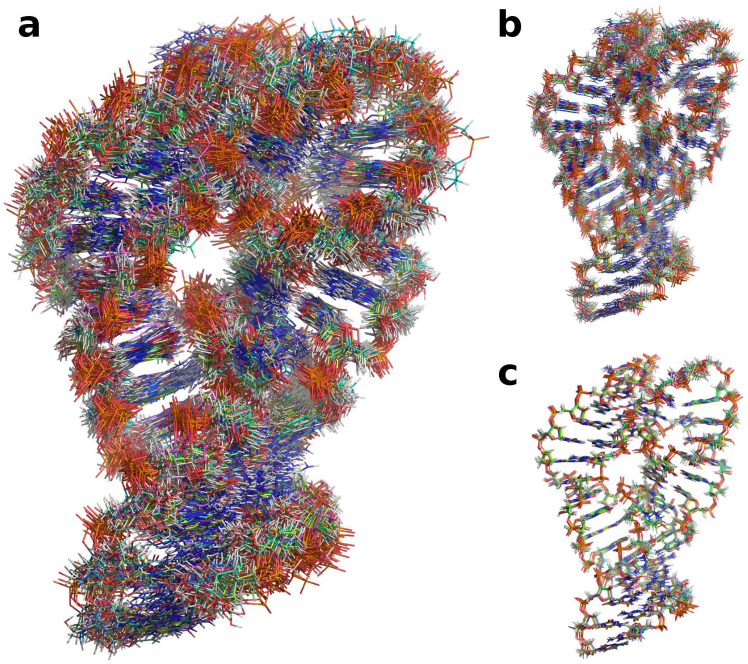

Figure S2: Overlays of representative structures from simulation of the twister ribozyme in the crystal environment. (a) Snapshots of each of the 12 monomers in the crystallographic unit cell taken every 20 ns. (b) Overlay of monomer structures averaged over the length of the 100 ns crystal simulation. (c) Snapshots taken every 20 ns of the trajectory generated by averaging over the coordinates of the 12 monomers within the unit cell. The overlay discussed in the main text (Figure 1) is an average over both time and monomer coordinates as that provides the more directly comparable structure to experiment.

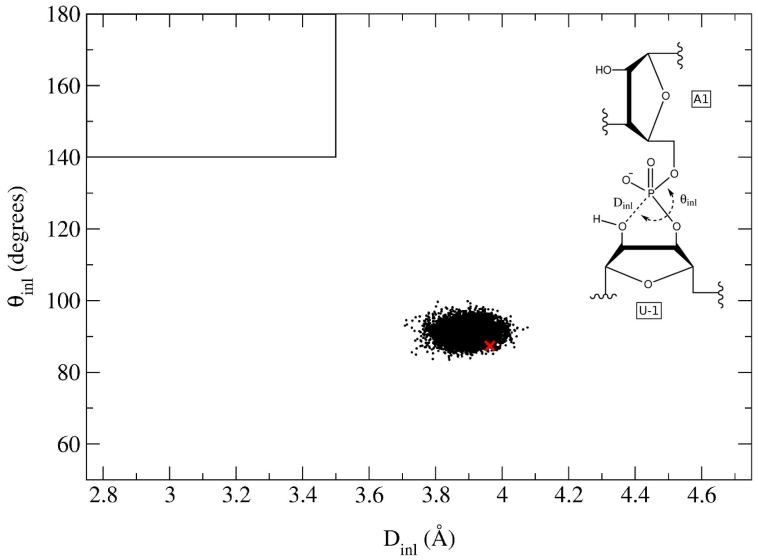

Figure S3: Scatter plot of in-line conformations for the crystal simulation. The black outlined region ($\theta_{inl} > 140°$ and $D_{inl} < 3.5$ Å) indicates active "in-line" conformations that favor catalysis. The red X indicates the average values of the nucleophile attack angle (91.6°) and distance (4.05 Å) for the double conformation of A1 in the deposited experimental structure (PDB: 4OJI[1]) with U-1:O2' modeled in.

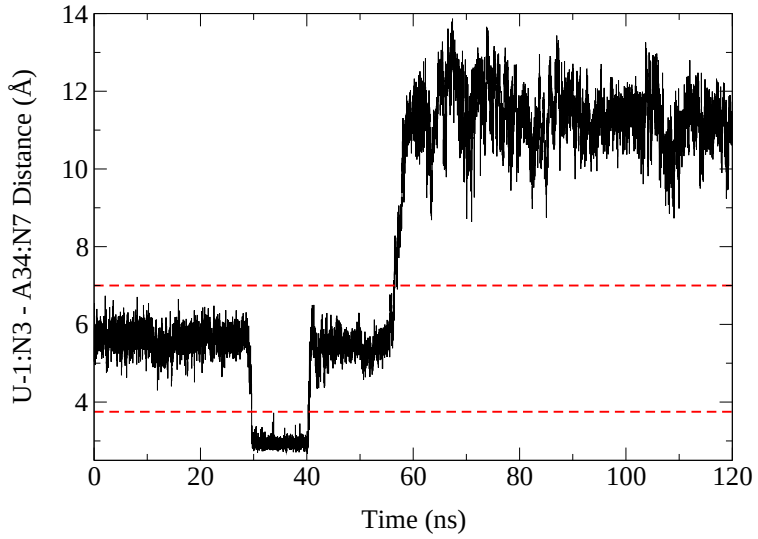

Figure S4: Time evolution of the U-1:N3 - A34:N7 distance, D_{stack}, showing the three stacking states of U-1. As indicated by the red dashed lines, the states are defined as follows: "Extruded" ($D_{stack} > 7.0$ Å), "Stacked" (3.75 Å$< D_{stack} < 7.0$ Å) and "Triple" ($D_{stack} < 3.75$ Å).

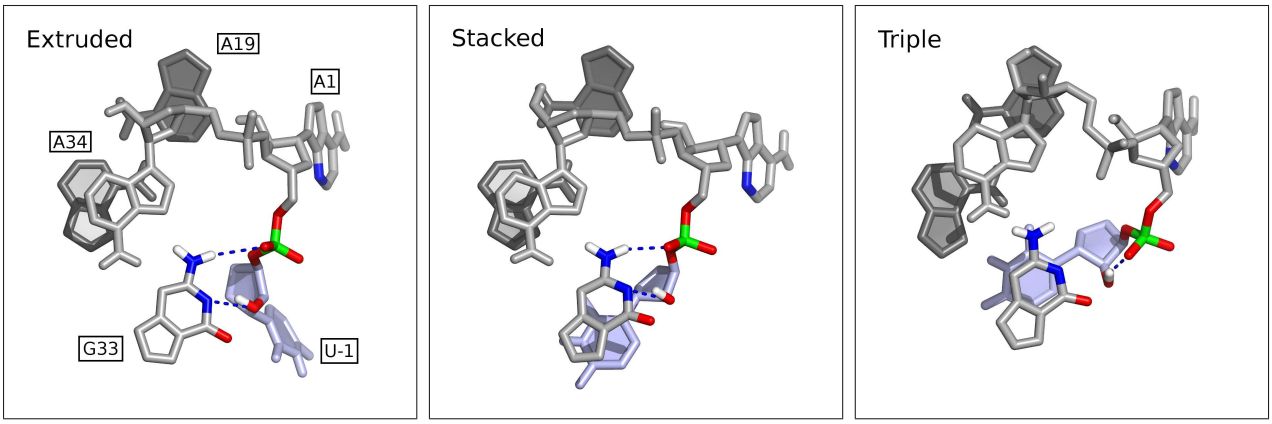

(a) G33N1$^-$ - Extruded (b) G33N1$^-$ - Stacked (c) G33N1$^-$ - Triple

Figure S5: Average structures from the restrained simulations exploring the conformational states of U-1 (light blue) are labeled as follows: (a) Extruded, (b) Stacked, and (c) Triple. The characteristic hydrogen bonding between G33 in its deprotonated form (G33N1$^-$) and either the scissile phosphate or the nucleophile is shown in dark blue.

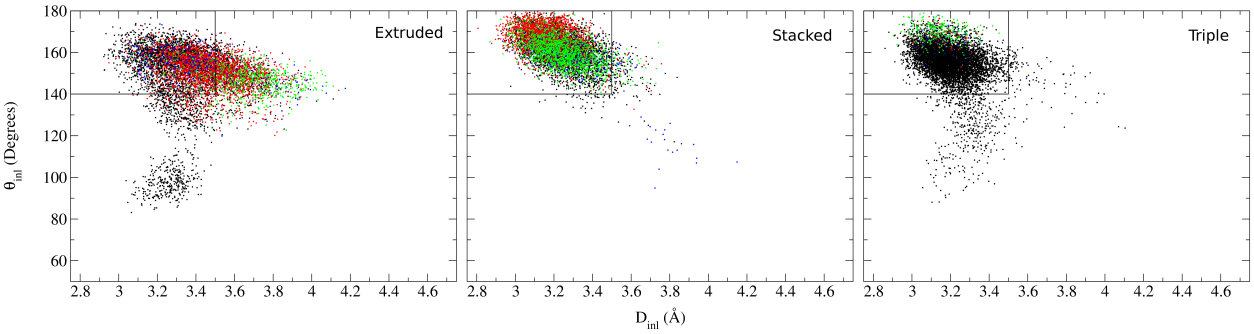

Figure S6: Nucleophile attack angle versus nucleophile-phosphate distance with G33 deprotonated (G33N1$^-$) and U-1 in each of the three conformational states (Extruded, Stacked, Triple). Clustering analysis is detailed in Fig. 5 of the main text. The black outlined region ($\theta_{inl} > 140^\circ$ and $D_{inl} < 3.5$ Å) and indicates active "in-line" conformations that favor catalysis.

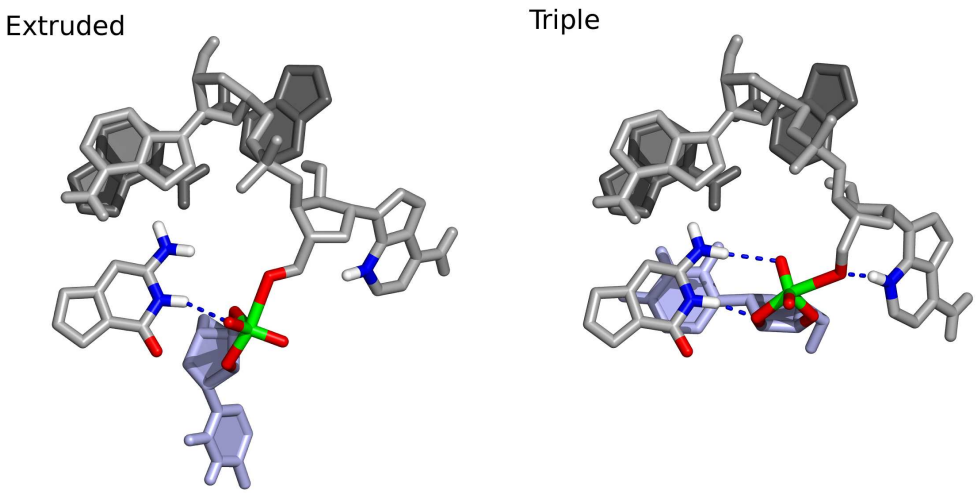

Figure S7: Representative structure of the proposed phosphorane transition state models along with the characteristic hydrogen bonding network, for both the U-1 extruded (a) and triple (b) states.

Table S1: Summary of free energy calculations for model nucleotide triplexes and each leg of the thermodynamic cycle presented in Figure 7. [a]Experimental pK_a values assigned to correspond with the free energy to deprotonate the N3 site for adenine[2] or the N1 site of guanine[3] in their respective triplexes. [b]The adjusted pK_a values after evenly distributing the residual -0.53 kcal/mol across all four microstates.

System	**ΔG (kcal/mol)**	**pK_a Shift**	**pK_a**	**Closed Cycle[b] pK_a**
CH_3-pU-**pA**-pA-CH_3	-68.62 $\pm$ 0.03	- -	1.5 $\pm$ 0.3[a]	- -
CH_3-pG-**pG**-pA-CH_3	-113.75 $\pm$ 0.11	- -	9.4 $\pm$ 0.2[a]	- -
${}_{AH^+}E_{BH} \rightarrow {}_{A}E_{BH}$	-61.84 $\pm$ 0.09	4.94 $\pm$ 0.07	6.44 $\pm$ 0.31	6.53 $\pm$ 0.31
${}_{AH^+}E_{BH} \rightarrow {}_{AH^+}E_{B^-}$	-115.54 $\pm$ 0.10	-1.31 $\pm$ 0.11	8.09 $\pm$ 0.23	7.99 $\pm$ 0.23
${}_{AH^+}E_{B^-} \rightarrow {}_{A}E_{B^-}$	-60.27 $\pm$ 0.09	6.08 $\pm$ 0.07	7.58 $\pm$ 0.31	7.48 $\pm$ 0.31
${}_{A}E_{BH} \rightarrow {}_{A}E_{B^-}$	-114.51 $\pm$ 0.10	-0.56 $\pm$ 0.11	8.84 $\pm$ 0.23	8.94 $\pm$ 0.23

References

(1) Liu, Y.; Wilson, T. J.; McPhee, S. A.; Lilley, D. M. J. *Nature Chem. Biol.* **2014**, *10*, 739–744.

(2) Kapinos, L. E.; Operschall, B. P.; Larsen, E.; Sigel, H. *Chem. Eur. J.* **2011**, *17*, 8156–8164.

(3) Verdolino, V.; Cammi, R.; Munk, B. H.; Schlegel, H. B. *J. Phys. Chem. B* **2008**, *112*, 16860–16873.